

FIFTH INTERNATIONAL CONGRESS ON SOUND AND VIBRATION

DECEMBER 15-18, 1997  
ADELAIDE, SOUTH AUSTRALIA

# ANALYSIS AND VISUALIZATION OF ROOM ACOUSTIC CHAOS

*Yoh-ichi FUJISAKA* <sup>(1)</sup>, *Mikio TOHYAMA* <sup>(1)</sup>, and *Akira SUGIMURA* <sup>(2)</sup>

(1) *Kogakuin University*  
(2) *Konan University*

This paper analyzes the chaotic characteristics of irregular systems using both wave theory and ray theory. In ray theory, we visualize the chaotic properties of the ray propagation trajectories in a chaotic wave field. We found that the trajectory of the billiard problem with a stadium boundary condition has the same sensitivities to the initial conditions as does the mapping process on a logistic map does. In wave theory, we investigate the distribution statistics of the eigenvalues and the correlation dimension of the higher-eigenmodes in an irregular system by using the Finite Element Method (FEM). We clarify the relationship between the curvature of the stadium boundary and the statistical degrees of freedom of the wave field. The eigenvalue spacing statistics were estimated by  $\Gamma$  distributions with fractional freedoms between 1 and 2.

## 1 INTRODUCTION

In a 2-dimensional region surrounded by the boundary of an irregular shape, the trajectory of a sound ray is unstable because of chaotic motion <sup>[1]</sup>. According to wave theory, the spacing distribution of the neighboring eigenvalues of an irregular system does not degenerate due to the repulsion effect, but rather follows a Wigner distribution <sup>[2][3]</sup>. Furthermore, the pressure field in higher modes of stadium shape shows a random pattern. But not all of these are random; some of them show patterns so-called scar patterns <sup>[4]</sup> which are left over from the classical orbits.

This paper discusses the chaotic properties of a sound field in a stadium-shaped region from the viewpoints of both ray theory and wave theory. In ray theory we calculate the sensitivity to the initial condition. We consider the billiard problems as a mapping of a sort that is a nonlinear initial value problem, and compare the behavior of orbits of the regular systems with those of the stadium. In wave theory, on the other hand, we found the eigenvalues and eigenmodes by using the Finite Element Method (FEM). We then analyze the eigenvalues and the eigenmodes to investigate the spacing statistics of the neighboring eigenvalues and the pressure distributions of the eigenfunctions.

## 2 RAY PROPAGATION

We investigated the propagations of a single ray under several boundary conditions. Figure 1 shows the ray propagation in several boundaries after 100 reflections. We can see that the trajectories are regular in the regular systems, such as the rectangle, the circle, and the ellipse. The trajectory becomes irregular in a stadium, however.

### 3 SENSITIVITIES TO INITIAL CONDITIONS

Chaotic signals have strong sensitivities to the initial conditions. This implies that the difference between two initial conditions becomes significant after several times, even if the difference is very small at the beginning. This property can be found in the ray propagation is considered a sort of mapping process as the logistic map [5]. To extract the chaotic properties in a stadium boundary, we consider two rays propagating under several boundary conditions. The difference between their initial directions is very small (Fig.2). We calculated their propagation after 40 reflection times. The calculations are carried out for 30 different initial conditions. Figure 3 shows the distance of the two rays for the 30 conditions where the horizontal axis indicates reflection times and the vertical axis indicates the difference between 2 rays. The differences linearly increase in the regular systems such as the rectangle, the circle, and the ellipse. However, in the stadium case, the difference increases exponentially as we see in Fig. 4. The chaotic propagation in irregular systems implies that it is not meaningful to calculate higher reflections of more than 20 times to predict room acoustics in an irregular shaped boundary including the curve boundary.

### 4 ANALYSIS IN WAVE FIELD

We considered the eigenvalue problem for two types of boundaries: a stadium and a rectangle. The wave function  $\psi$  satisfies

$$\frac{\partial^2 \psi}{\partial x^2} + \frac{\partial^2 \psi}{\partial y^2} = -\left(\frac{\omega}{c}\right)^2 \psi. \quad (1)$$

To solve Eq. 1 for the stadium boundary, we used FEM. The eigenvalues for the rectangular boundary are given by

$$\omega_{lm} = c \sqrt{\left(\frac{l\pi}{L_x}\right)^2 + \left(\frac{m\pi}{L_y}\right)^2}, \quad (2)$$

( $\omega_{lm}$ : eigenfrequency,  $c$ : sound speed)

where  $L_x$  and  $L_y$  indicate the lengths of the rectangular sides.

#### 4.1 SPACING STATISTICS

The spacing statistics for eigenvalues also characterize the sound fields. We analyzed the spacing statistics with 300 eigenvalues. Figure 5(a) indicates the spacing histogram for the rectangular boundary, and Fig. 5(b) indicates that for the stadium boundary where the horizontal axis indicates the normalized eigenvalue spacing  $k$  and the vertical axis indicates the histogram. The statistics for the rectangular boundary show an exponential distribution due to degenerate, while that for the stadium boundary shows a Wigner distribution. These distributions can be estimated by the  $\Gamma$  distribution with 1 and 2 degrees of freedom. Next, we consider a stadium that has a curvature which is represented by  $x^i + y^i = r^i$ . Figure 6 shows the spacing distribution of the eigenvalues when  $i=3, 5, 7,$  and  $15$ . We can see that these distributions follow the  $\Gamma$  distribution [6] which is given by

$$P(x, n) = \frac{\lambda^n x^{n-1}}{\Gamma(n)} e^{-\lambda x}, x > 0 \quad (3)$$

where  $n$  denotes the degrees of freedom. The degree of freedom is almost 1 and the distribution is similar to that for the rectangular case (regular systems) when the curvature is 15.

The distributions of the eigenvalues of random matrices <sup>[7]</sup> are changed from the exponential distribution to a Wigner one as the power ratio of the diagonal elements to non-diagonal components increases. Here, we denote

$$E = \begin{pmatrix} a_{11} & & & A \\ & a_{22} & & \\ & & \dots & \\ A & & & a_{nn} \end{pmatrix} \quad (4)$$

and

$$d = \frac{\langle D^2 \rangle}{\langle A^2 \rangle}. \quad (5)$$

Figure 7 shows the spacing statistics for eigenvalues of the random matrices. We can reconfirm that the spacing distribution can also be estimated by the  $\Gamma$  distribution with the degrees of freedom  $n$ .

## 4.2 EIGENFUNCTION STATISTICS

We try to analyze the characteristics of the eigenfunctions under the rectangular and stadium boundaries. We examined the spatial distribution statistics (sampling statistics) for these boundaries. Histograms of the samples  $\psi$  in a higher eigenmode for the rectangular and stadium boundaries are presented in Figs.8(a) and 8(b), respectively. The horizontal axis indicates the sample value of  $\psi$  and the vertical axis indicates the probability density. The rectangular boundary provides a distribution that is concentrated around the average of 0. The stadium boundary, on the other hand, provides a distribution that corresponds to a Gaussian distribution that has the random property.

## 4.3 DIMENSIONAL ANALYSIS

In the previous section, we confirmed that the distribution for the higher eigenfunction follows the Gaussian distribution for the stadium case. In this section, we will analyze the correlation dimension for the higher mode. Suppose that  $Z(x)$  is a random variable. The dimensional analysis composes a vector  $V(x)$  for the embedding dimension  $n$  by using the distance displacement  $\delta$  as shown in the following,

$$V(x) = \{z(x), x(x + \delta), \dots, z(x + (n - 1)\delta)\} \quad (6)$$

and

$$\xi_i = (x_i, x_{i+1}, \dots, x_{i+n-1}) \quad (7)$$

We count the number of the pairs of the sample point located within a certain distance under the condition that the embedding dimension is  $n$ . This number is written as

$$C(r) = \lim_{N \rightarrow \infty} \frac{1}{N^2} \sum_{i,j=1, i \neq j} \theta(r - |\xi_i - \xi_j|). \quad (8)$$

( $\theta$  is the unit step function.)

The correlation dimension  $\nu$  is given by

$$C(r) \sim Ar^\nu \quad (9)$$

at every embedding dimension  $n$ . We define the correlation dimension as the limit which is obtained as the embedding dimension becomes infinite. If the sequence is a random noise, the correlation dimension becomes infinite. If the sequence has some correlation, the correlation dimension converges a fixed value. We took the eigenfunction's intensity on the central axis along the  $x$  axis as shown in Fig. 9. Figure 10 shows the correlation dimension reaches 1.5 after the embedding dimension is larger than 2.

## 5 CONCLUSIONS

We have investigated the chaotic properties of a stadium field from the viewpoints of both ray theory and wave theory. In ray theory, the chaotic property is represented by the sensitivities to the initial conditions. In wave theory, we first used FEM to calculate the eigenvalues and eigenmodes which were then statistically analyzed. We considered the statistical properties of eigenfunctions for the stadium boundary. We reconfirmed that the eigenvalue spacing follows a Wigner distribution, and the correlation dimension of the higher mode is 1.5. The spatial distribution of higher modes for the stadium boundary looks random; however, we can surmise that the pressure distribution of a eigenfunction as the diffuse sound field might have a lower dimension (degrees of freedom). For the stadium boundaries of different curvatures, the degree of freedom of  $\Gamma$  distributions which estimate the eigenvalue spacing statistics have been found to be between 1 and 2. We can guess that even the complicated phenomena in the stadium boundary has only 2 degrees of freedom.

## ACKNOWLEDGMENT

The authors would greatly appreciate Prof. Dr. M.R.Schroeder's valuable discussions and suggestions about section 4.1.

## References

- [1] M.V. Berry, *Eur. J. Phys.* **2**, 91 (1981).
- [2] S.W. McDonald and A.N. Kaufman, *Phys. Rev. Lett.* **42**, 1189 (1979).
- [3] R.H. Lyon, *J. Acoust. Soc. Am.* **45**, 545 (1969).
- [4] S.W. McDonald and A.N. Kaufman, *Phys. Rev.* **37**, 3067 (1988).
- [5] Robert C. Hilborn, "Chaos and Nonlinear Dynamics", Oxford University Press 20 (1994).
- [6] H. J. Larson, "Introduction to Probability Theory and Statistical Inference", third edition, Wiley series in probability and mathematical statistics, 200 (1982).
- [7] M. Metha, "Random Matrices", Academic Press (1991).
- [8] N. Gershenfeld, "Directions in Chaos", Ed. by Hao Bai-lin, World Scientific, 310 (1988).

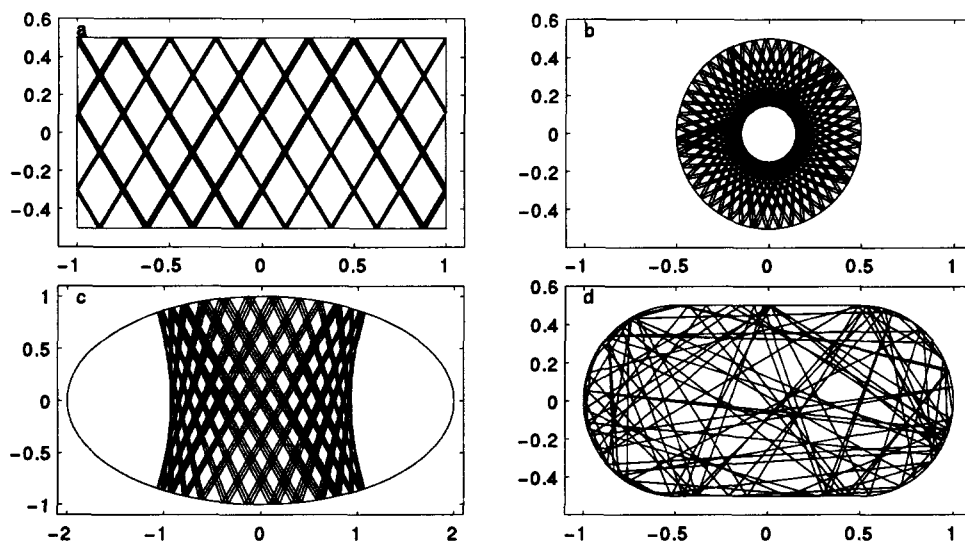


Figure 1: Ray propagation using a single ray: (a) rectangle, (b) circle, (c) ellipse and (d) stadium

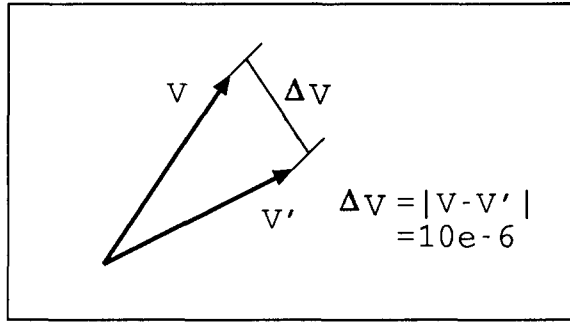


Figure 2: Initial condition for investigating sensitivities of ray propagation in several boundary shapes

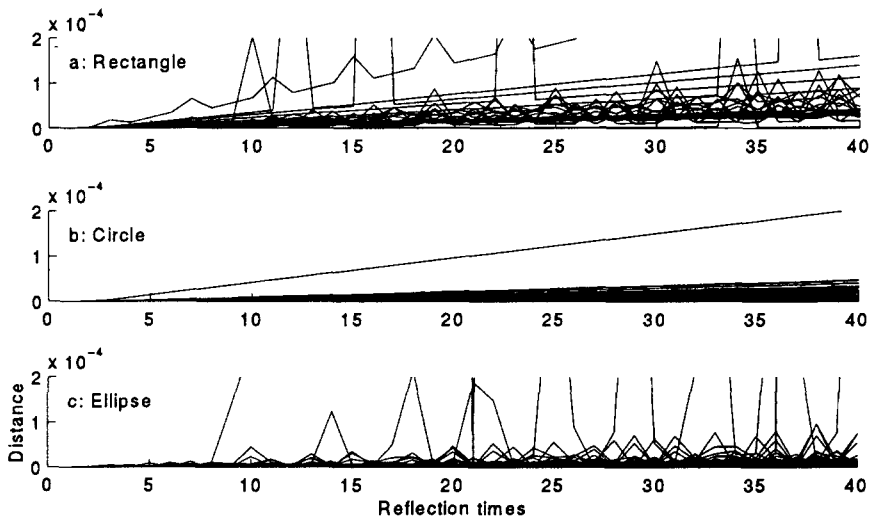


Figure 3: Sensitivity to the initial conditions for regular systems (Distance: distance between two rays on the reflection points)

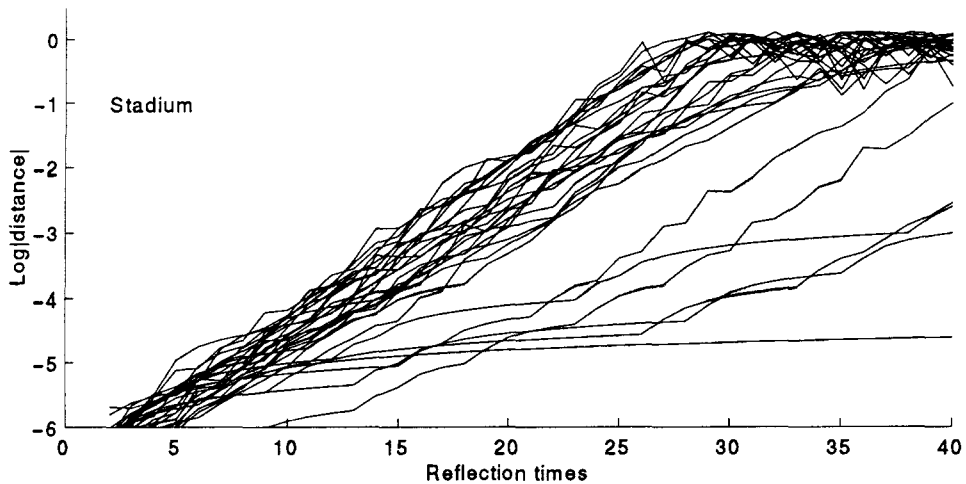


Figure 4: Sensitivity to the initial conditions for a stadium boundary

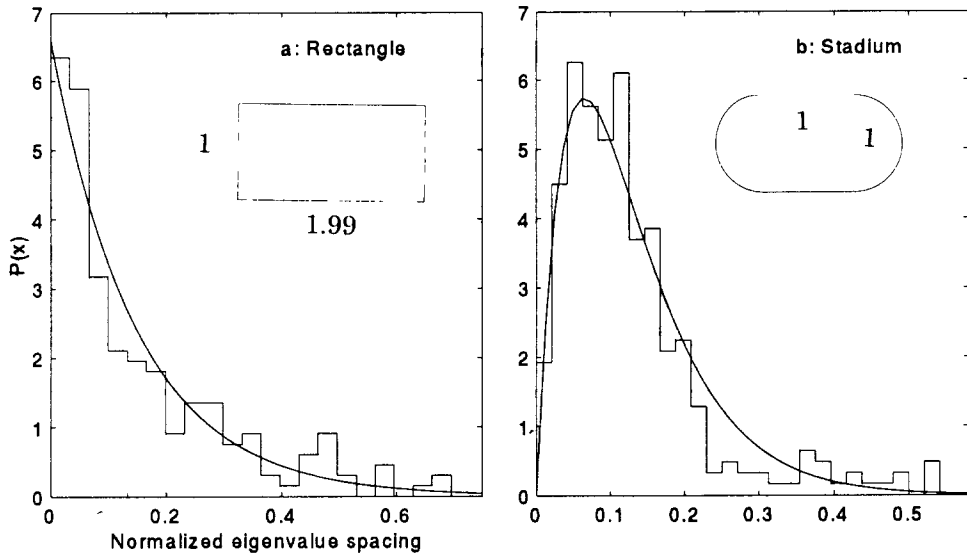


Figure 5: Spacing statistics of the neighboring eigenvalues (a) rectangle: smoothing line indicates Poisson distribution:  $(1/\rho)\exp(-(x - \mu)/\rho)$ .  $\mu \simeq 0.16, \rho \simeq 0.18$ ; (b) stadium: smoothing line indicates Wigner distribution:  $(4x/\mu^2)\exp(-x^2/\mu)$   $\mu \simeq 0.13$

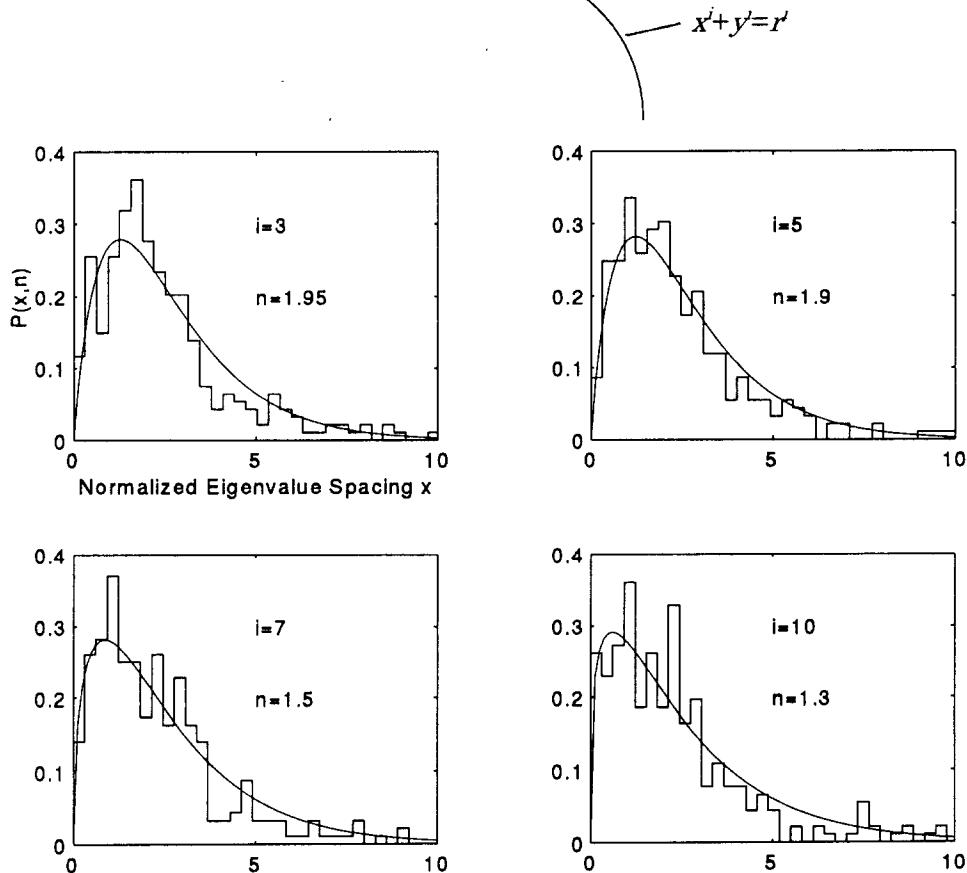


Figure 6: Eigenvalue spacing statistics for stadium with different curvatures;  $n$ : degrees of freedom of the  $\Gamma$  distribution

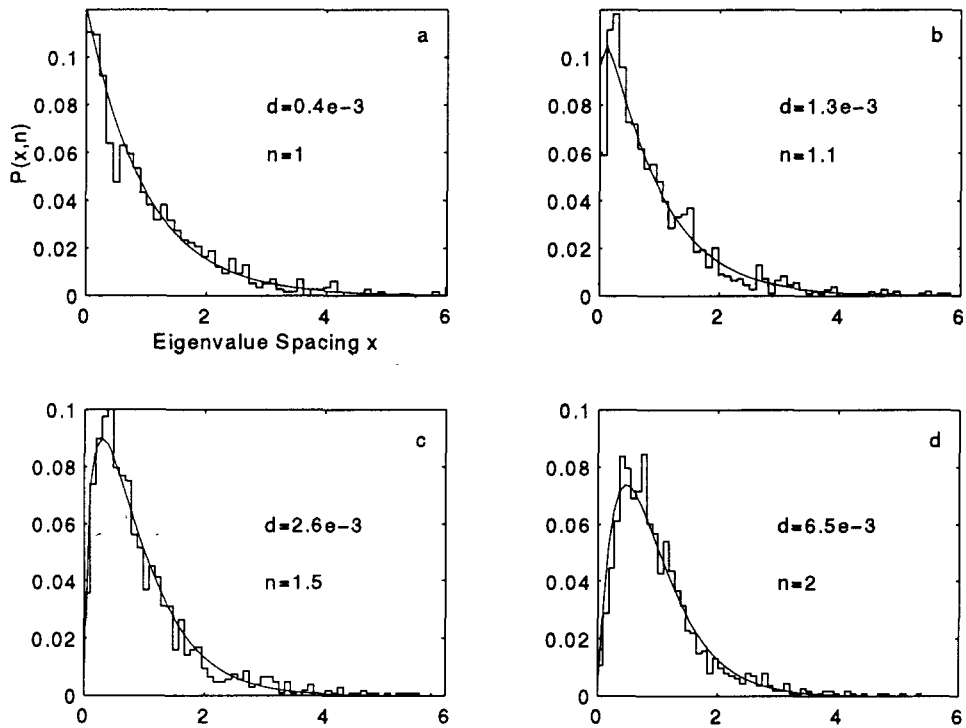


Figure 7: Eigenvalue spacing statistics for random matrices where  $d$  is the power ratio of the diagonal elements to non-diagonal components and  $n$  denotes the degrees of freedom of the  $\Gamma$  distribution

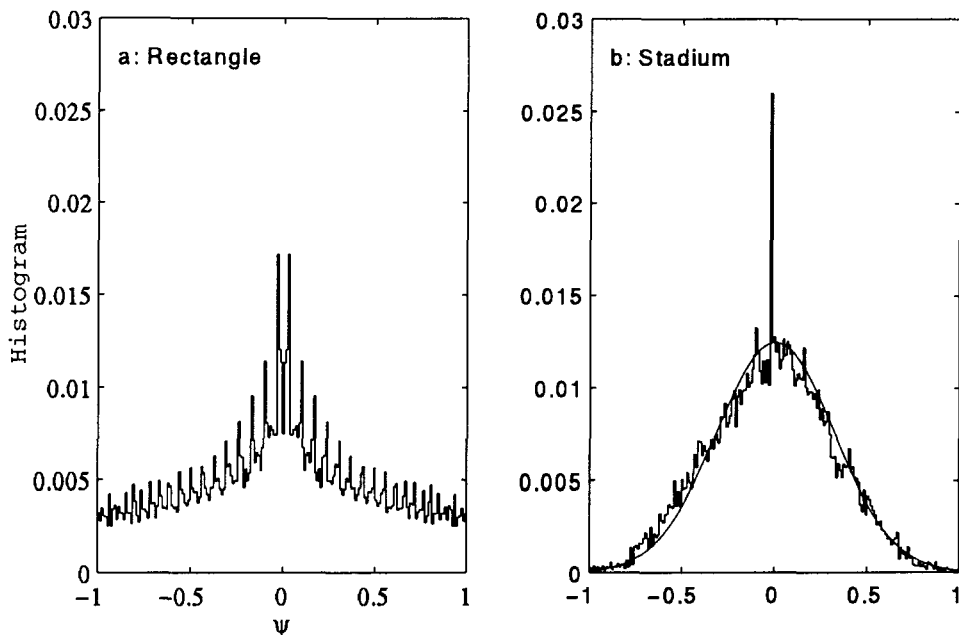


Figure 8: Sampling histograms of the sound pressure field of a higher mode (a): rectangle, (b): stadium

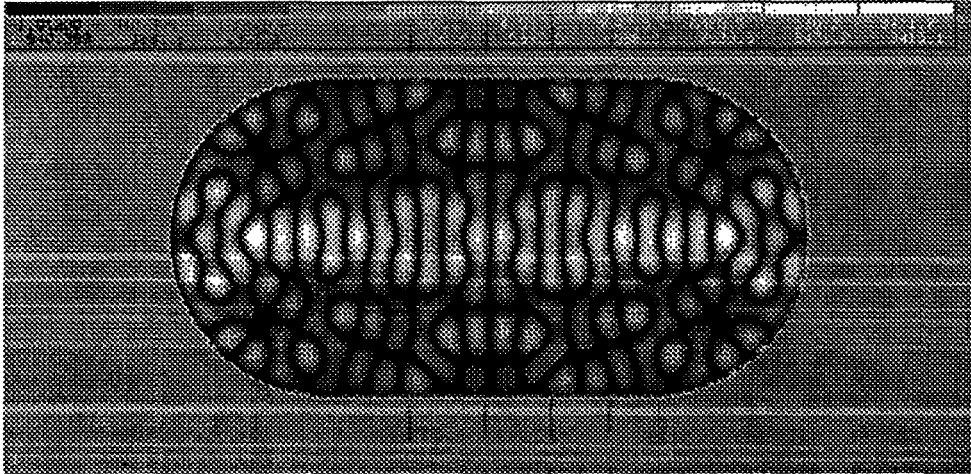


Figure 9: An example of higher order mode of the stadium boundary

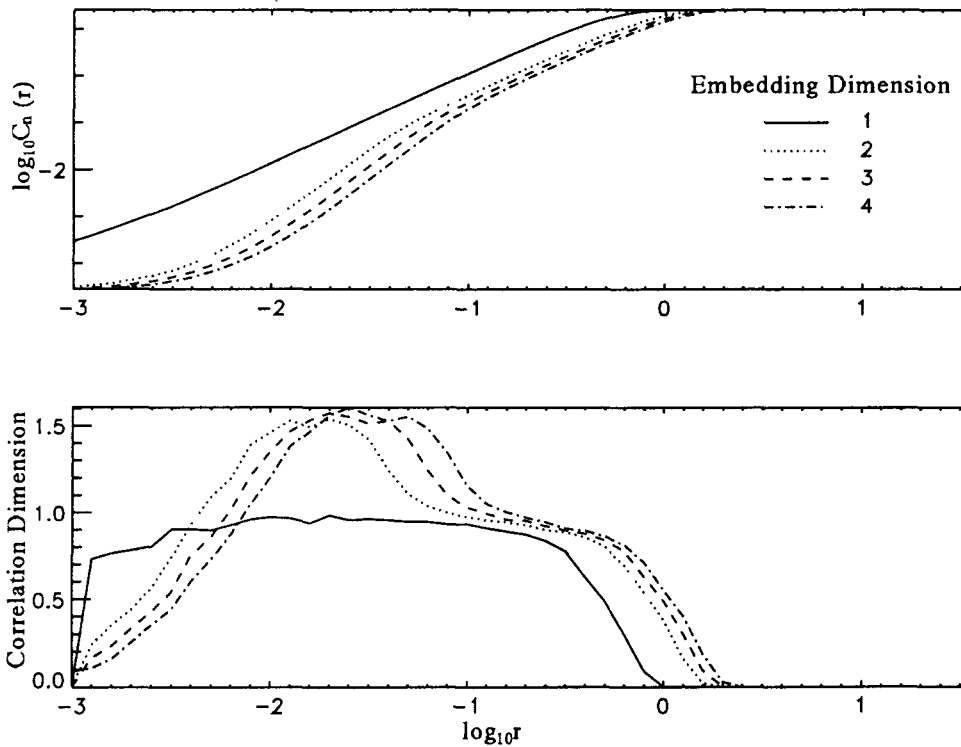


Figure 10: Correlation dimension analysis of sound intensity distribution on the central axis along the  $x$  in Fig.9